GEOPHYSICAL RESEARCH LETTERS., VOL. 29, NO. 19, 1901, doi:10.1029/2002GL015112, 2002

Observation of dust and anthropogenic aerosol plumes in the Northwest Pacific with a two-wavelength polarization lidar on board the research vessel Mirai

Nobuo Sugimoto, Ichiro Matsui, and Atsushi Shimizu
National Institute for Environmental Studies, Japan

Itsushi Uno
Research Institute for Applied Mechanics, Kyushu University, Japan

Kazuhiro Asai
Tohoku Institute of Technology, Japan

Tatsuo Endoh
Institute of Low Temperature Science, Hokkaido University, Japan

Teruyuki Nakajima
Center for Climate System Research, University of Tokyo, Japan

Received 13 March 2002; revised 22 May 2002; accepted 18 June 2002; published 2 October 2002.

[1] Dust and anthropogenic aerosol plumes from the Asian continent were observed in the Northwest Pacific (32.0° to 38.0°N, 146.5°E) with a two-wavelength polarization lidar on board the research vessel Mirai during the MR01-K02 cruise (May 14 to 28, 2001). Dust aerosols were identified from the aerosol depolarization ratio at 532 nm and the ratio of the backscattering coefficient at 1064 nm and 532 nm. High aerosol density air masses with a low depolarization ratio and a small wavelength ratio (indicating small particle size) were also detected in the plume. The distribution patterns of the dust and the spherical aerosols were conceptionally explained by the model prediction for dust and sulfate with the Chemical Weather Forecast System (CFORS). Aerosols with large particle size but with low depolarization ratio were also observed in between the layers of dust and sulfate. This indicates that the aerosols were possibly an internal mixture of dust and sulfate. *INDEX TERMS:* 0305 Atmospheric Composition and Structure: Aerosols and particles (0345, 4801); 0345 Atmospheric Composition and Structure: Pollution—urban and regional (0305); 3337 Meteorology and Atmospheric Dynamics: Numerical modeling and data assimilation; 3360 Meteorology and Atmospheric Dynamics: Remote sensing. **Citation:** Sugimoto, N., I. Matsui, A. Shimizu, I. Uno, K. Asai, T. Endoh, and T. Nakajima, Observation of dust and anthropogenic aerosol plumes in the Northwest Pacific with a two-wavelength polarization lidar on board the research vessel Mirai, *Geophys. Res. Lett.*, *29*(19), 1901, doi:10.1029/2002GL015112, 2002.

1. Introduction

[2] Anthropogenic aerosols and mineral dust in Eastern Asia and the Northwest Pacific are considered to significantly affect radiative forcing and the global atmospheric environment [*Jaffe et al.*, 1999; *Husar et al.*, 2001]. Thus, the outflow of desert dust and anthropogenic aerosol from Eastern Asia to the Pacific is the target of the Asian Pacific Regional Aerosol Characterization Experiment (ACE-Asia) of the International Global Atmospheric Chemistry Program (IGAC). As a part of the Japanese activities in ACE-Asia, we conducted lidar observation in the Pacific on cruise MR01-K2 of the research vessel Mirai (May 14 to 28, 2001) at the same time with various sampling measurements and physical measurements. In this paper, we report on the aerosol plumes observed with the lidar during the cruise.

[3] The lidar we used in the observation is a two-wavelength, Mie-scattering lidar (1064 nm, 532 nm) with a depolarization measurement capability at 532 nm [*Sugimoto et al.*, 2000, 2001]. We analyzed the characteristics of the observed aerosols using the aerosol depolarization ratio and the ratio of backscattering coefficients at 1064 nm and 532 nm. The aerosol depolarization ratio is useful for identifying dust aerosols because it indicates nonsphericity of the scatterer [*Browell et al.*, 1990; *Murayama et al.*, 2001]. The wavelength ratio is useful for obtaining aerosol particle size information. We also used the model prediction with the real-time Chemical Weather Forecast System (CFORS) developed at Kyushu University [*Uno et al.*, 2001b] to identify aerosol types.

2. Observations and Modeling

[4] Lidar observations were performed continuously during the whole MR01-K02 cruise of R/V Mirai. Figure 1 shows the cruise track. The lidar employs a flash-lamp-pumped Nd:YAG laser as a light source that generates the fundamental output at 1064 nm and the second harmonic at 532 nm. The transmitted energy is typically 100 mJ per pulse at 1064 nm and 50 mJ per pulse at 532 nm. The pulse repetition rate is 10 Hz. The receiver telescope has a diameter of 25 cm. It has three detection channels to receive

0094-8276/02/2002GL015112$05.00

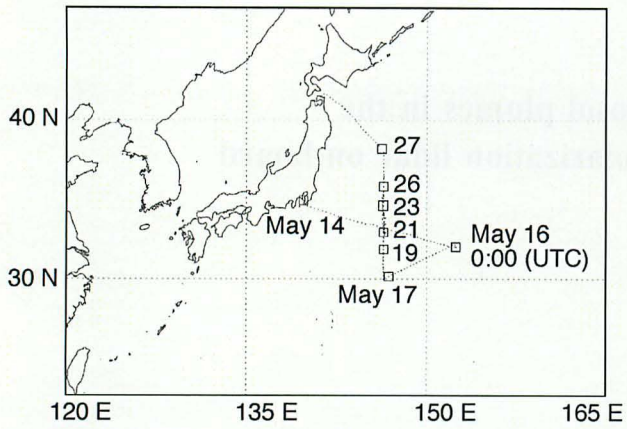

Figure 1. Cruise tracks of MR01-K02 of R/V Mirai.

the lidar signals at 1064 nm and two polarization components at 532 nm. An analogue-mode avalanche photo diode (APD) is used for 1064 nm, and photomultiplier tubes (PMTs), for 532 nm. The lidar system was installed in a container with a glass window on the roof, and it was operated continuously regardless of weather [*Sugimoto et al.*, 2000]. Automated sky-radiometer observation was conducted by Hokkaido University throughout the cruise. Radiosondes were launched twice a day (0900 and 2100 JST) by the Japan Marine Science and Technology Center (JAMSTEC). Also, surface meteorological parameters were recorded routinely.

[5] We compared the observation with the real-time Chemical Weather Forecast System (CFORS). The CFORS was developed based on a 3D on-line regional scale chemical transport model fully coupled with the Regional Atmospheric Modeling System (RAMS). One of the main purposes of this CFORS is to understand the regional transboundary pollution and to schedule and design an operational field monitoring campaign during the TRACE-P (TRAnsport and Chemical Evolution over the Pacific) and the ACE-Asia intensive observations scheduled during the spring of 2001. The simulation domain adopted is centered at 25°N, 115°E. The horizontal grid consists of 100 by 90 grid points, with a resolution of 80 km. In the vertical dimension, the domain is divided into 23 layers. The present CFORS system includes the following chemical transport species: SO2/Sulfate, DMS, volcano tracer, megacity urban plume, black carbon, organic carbon, sea salt, CO, hydrocarbons, and Radon and mineral dust (12 bins). Concept of dust transport and details of CFORS can be found in *Uno et al.* [2001a, 2001b].

3. Results and Discussion

[6] Figure 2 shows the results of the lidar observation throughout the cruise (May 14–27). (a) Cloud base height and apparent cloud top height, (b) aerosol backscattering coefficient at 532 nm, (c) aerosol depolarization ratio at 532 nm, (d) the ratio of the aerosol backscattering coefficients at 1064 nm to 532 nm, and (e) aerosol optical depth from the sea level to 6 km altitude. The lidar data were analyzed in the same manner as described in *Sugimoto et al.* [2001]. The threshold method was applied to detect clouds to the 15-min averaged lidar profiles. In the aerosol analysis, the profiles having clouds below 3 km were removed and the geometrical form factor correction was applied. Aerosol backscattering coefficient was obtained with the two-component backward inversion method [*Fernald*, 1984] with an assumption of constant lidar ratio (or extinction-to-backscatter ratio), S1. We set the boundary condition above 6 km or at the highest height below the clouds when there were clouds between 3 and 6 km. We assumed S1 = 50 sr both at 532 nm and 1064 nm based on the climatological analysis for tropospheric aerosols over Tsukuba, Japan [*Sasano*, 1996]. The recent observations with a Raman lidar and a high-spectral-resolution lidar also showed that S1 is 40–55 at 532 nm for Asian dust [*Liu et al.*, 2002]. We tested S1 = 40 sr and 60 sr to estimate the error introduced by the assumption of S1. The difference from the S1 = 50 sr case was about +16% and −11% at 1 km height. We applied non-zero boundary values for aerosol backscattering when the inversion result gives negative backscatter coefficient in the lower altitude. The boundary values were determined iteratively. The Mie to Rayleigh scattering ratio at the boundary was less than 0.5 in the most cases. In the inversion of the 1064 nm data, we used the method similar to that developed for a space-borne lidar [*Liu et al.*, 2000; *Sugimoto et al.*, 2001]. In this method, the boundary conditions were determined from the signals at 532 nm,

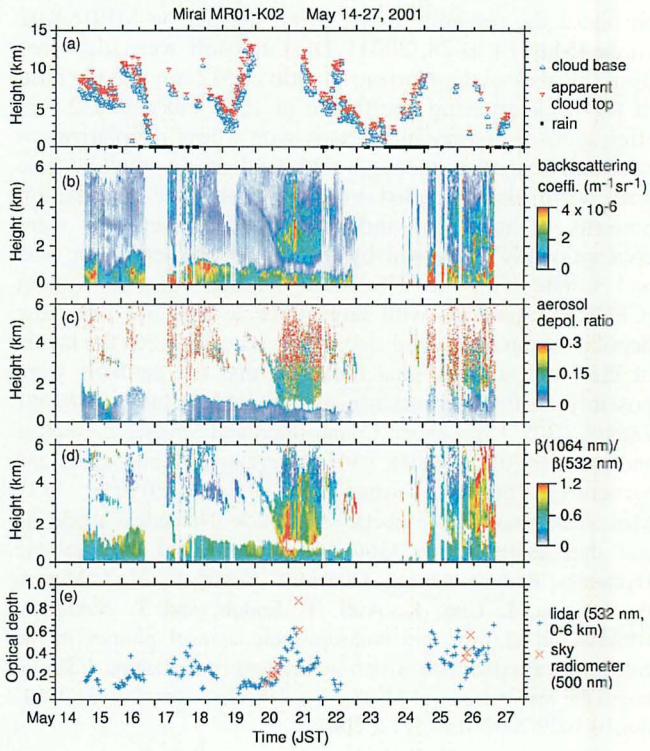

Figure 2. Results of the lidar observation during the cruise. (a) Cloud base height and apparent cloud top height, (b) aerosol backscattering coefficient at 532 nm, (c) aerosol depolarization ratio at 532 nm, (d) the ratio of the aerosol backscattering coefficients at 1064 nm to 532 nm, and (e) aerosol optical depth from the sea level to 6 km altitude with an assumption of S1 = 50. Optical depth obtained with a sky-radiometer is also indicated in (e). Areas with insufficient signal-to-noise ratio were set to white.

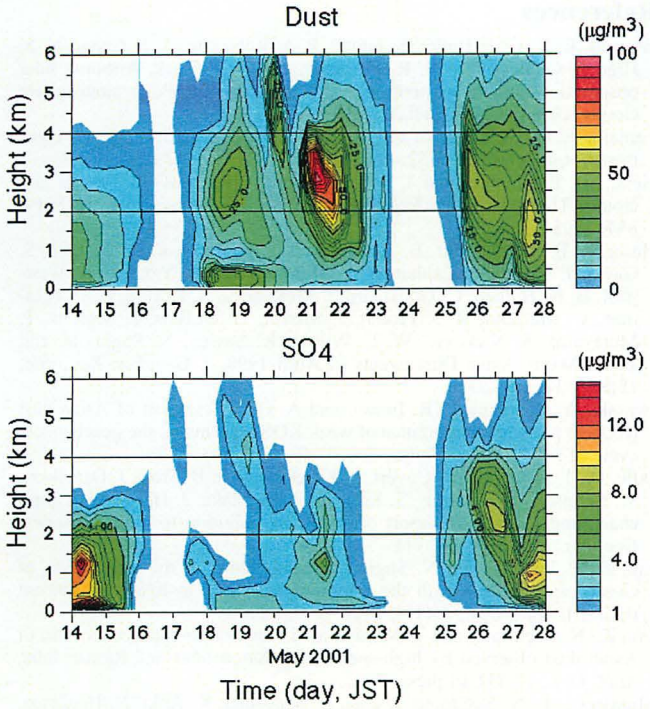

Figure 3. Time-height indication of dust and sulfate along the ship track predicted with the CFORS chemical transport model.

because the signal-to-noise ratio of the Rayleigh scattering signal at 1064 nm was not sufficiently high. The boundary values for Rayleigh and Mie scattering were separately estimated when non-zero boundary values were used in the inversion at 532 nm. We assumed a wavelength dependence of aerosol backscattering of λ^{-1} at the boundary.

[7] Aerosol depolarization ratio (ADR) or particle depolarization ratio (PDR) [*Browell et al.*, 1990] was derived from the total-to-Rayleigh backscattering ratio (BR), and the total depolarization ratio (TDR), from the following equation [*Liu et al.*, 2002].

$$\mathrm{ADR} = \frac{\mathrm{TDR}(\mathrm{BR} + \mathrm{BR} \times \mathrm{MDR} - \mathrm{MDR}) - \mathrm{MDR}}{\mathrm{BR} - 1 + \mathrm{BR} \times \mathrm{MDR} - \mathrm{TDR}} \quad (1)$$

where MDR is the molecular depolarization ratio. We used MDR = 0.014 in this work. ADR is sensitive to errors when the backscattering coefficient is small. We masked in Figure 2c the areas where the statistical error was large. Errors in wavelength ratio are introduced from the errors in backscattering coefficients at 532 nm and 1064 nm. The largest source of the error in 1064 nm in this work is the error in the boundary condition. Errors as large as 50% may be included in the absolute value. The relative error in a profile is smaller. The areas where the statistical error was large were masked in Figure 2.

[8] Optical depth at 500 nm observed with a sky-radiometer is also plotted in Figure 2e. As seen in Figure 2a, middle and high altitude clouds are often observed, and cloud free daytime condition was not available except for May 20 and 26. The optical depth up to 6 km obtained from the lidar agrees well with the optical depth observed with the sky-radiometer. This indicates that the assumption of lidar ratio of 50 is acceptable.

[9] Plumes of aerosols were observed from 1400 JST May 20 to 2300 JST May 21, and 2000 JST May 25 to 2200 JST May 26. The aerosol depolarization ratio (ADR) reveals that the plumes contain dust aerosols. The two-wavelength ratio indicates that particle size is relatively large in the plumes. This is consistent with the fact that dust aerosol particles are generally large. In the atmospheric boundary layer up to 0.6–1.5 km, ADR was generally low. However, it was slightly high on May 14–15 and May 18–22.

[10] A layered structure is seen in the aerosol plume observed on May 26. ADR is large above 1.6 km, but ADR is relatively small in the middle layer (0.8–1.6 km). It is especially low in the boundary layer below 0.8 km. The wavelength ratio is relatively small in the middle layer. This indicates relatively small spherical aerosols were dominant in the middle layer. In the boundary layer, spherical liquid sea salt was probably dominant.

[11] Figure 3 shows the time-height cross section of dust and sulfate predicted by CFORS along the path of R/V Mirai. In Figure 3, the dust plumes on May 21 and May 26 were predicted by CFORS quite well. On May 21, a low-concentration sulfate plume was predicted at a lower altitude. On May 26, relatively high-concentration sulfate plumes were predicted in the same altitude range as the dust plumes with a slight delay. The observed structure of aerosol plumes shown in Figure 2 is conceptually explained with the CFORS prediction if we identify the observed spherical aerosols in the middle layer of the plume on May 26 as sulfate. Slightly high ADR in the boundary layer on May 18–21 is also conceptually explained by the high dust concentration in the CFORS prediction.

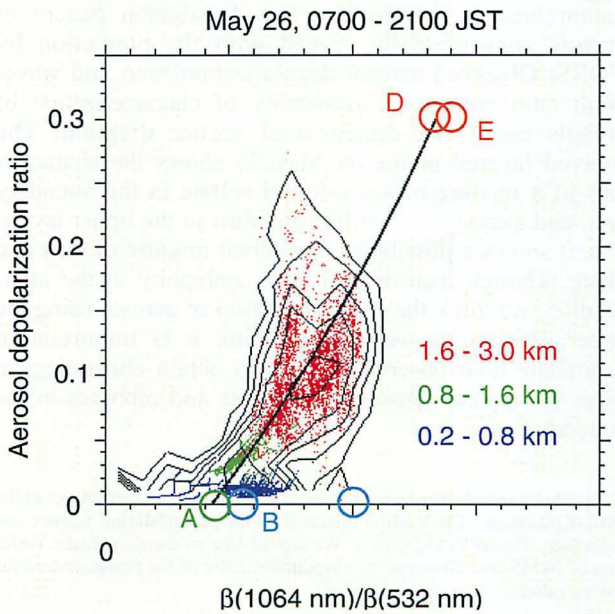

Figure 4. Scatter diagram of the aerosol depolarization ratio and the wavelength ratio for the aerosol plume observed on May 26. Open circles indicate calculated values using OPAC for (a) sulfate, (b) sea salt accumulation mode, (c) sea salt coarse mode, (d) dust (desert without water soluble), and (e) dust (mineral accumulation mode). ADR of dust was given arbitrarily in C and D. The line indicates theoretical curve for an external mixture of A and D.

[12] Figure 4 shows a scatter diagram of wavelength ratio and ADR in the plume observed during 0700–2100 JST on May 26. Three altitude regions are indicated in different colors. We used the data with sufficiently high backscattering coefficient (>2 $\sim 10^{-5}m^{-1}sr^{-1}$). It can be seen that the aerosols in the three different altitude region have different characteristics. The open circles in Figure 4 indicate theoretical values calculated for (A) sulfate, (B and C) sea salt, and (D and E) dust using OPAC model [*Hess et al.*, 1998]. We gave the ADR of 0.3 for the dust arbitrarily here, because ADR is not obtained from OPAC. The line in the figure indicates theoretical values for simple external mixture of A and D. Though these modeled values are dependent on various assumptions and contain large ambiguity especially for dust aerosols, Figure 4 shows a possibility of characterizing aerosols using observed wavelength ratio and ADR. From Figure 4 and the distribution pattern of the CFORS prediction, the aerosols in the boundary layer are most likely a mixture of sea salt and sulfate. The aerosols in the upper layers are probably a mixture of sulfate and dust. A part of data points in the upper layers falls on a line describing an external mixture. However, there are many data points in the low ADR side of the line. This may be explained by internal mixing of dust and sulfate [*Iwasaka et al.*, 1988]. Relative humidity observed with a radiosonde at 0900 May 26 was 60 to 65% at 0 to 1.2 km, 2.4 to 2.6 km, and 3.4 to 4.3 km, and 70 to 80% at1.6 to 1.8 km. In these high humidity regions, internal mixing possibly occurs.

4. Conclusion

[13] Plumes of dust and sulfate aerosols from the Asian continent were observed with the two-wavelength depolarization lidar in the Pacific. The distribution pattern of aerosols conceptionally agreed with the prediction by CFORS. Observed aerosol depolarization ratio and wavelength ratio indicates a possibility of characterization of aerosols using two-dimensional scatter diagram. The observed layered plume on May 26 shows the characteristics of a mixture of sea salt and sulfate in the boundary layer, and a mixture of sulfate and dust in the upper layers. Also, it shows a possibility of internal mixture of dust and sulfate. Though there is still large ambiguity in the interpretation, we think the characterization of aerosol using the scatter diagram is useful. We think it is important to accumulate lidar observation data to obtain climatological values for typical aerosol components and mixtures in the future studies.

[14] **Acknowledgments.** The lidar observation was carried out in the MR01-K02 cruise of R/V Mirai operated by the Japan Marine Science and Technology Center (JAMSTEC). We would like to thank Yasushi Yoshikawa of JAMSTEC who was the chief investigator of the cruise, and all the crew members.

References

Browell, E. V., C. F. Butler, S. Ismail, P. A. Robinette, A. F. Carter, N. S. Higdon, O. B. Toon, M. R. Schoeber, and A. F. Tuck, Airborne lidar observations in the wintertime Arctic stratosphere: Polar stratosphere clouds, *Geophys. Res. Lett.*, *17*, 385–388, 1990.

Fernald, F. G., Analysis of atmospheric lidar observations: Some comments, *Appl. Opt.*, *23*, 652–653, 1984.

Hess, M., P. Koepke, and I. Schult, Optical properties of aerosols and clouds: The software package OPAC, *Bull. Am. Meteor. Soc.*, *79*, 831–844, 1998.

Husar, R. B., D. M. Tratt, B. A. Schichtel, S. R. Falke, F. Li, D. Jaffe, S. Gasso, T. Gill, N. S. Laulainen, F. Lu, M. C. Reheis, Y. Chun, D. Westphal, B. N. Holben, C. Gueymard, I. McKendry, N. Kuring, G. C. Feldman, C. McClain, R. J. Frouin, J. Merrill, D. DuBois, F. Vignola, T. Murayama, S. Nickovic, W. E. Wilson, K. Sassen, N. Sugimoto, and W. C. Malm, Asian Dust events of April 1998, *J. Geophys. Res.*, *106*, 18,317–18,330, 2001.

Iwasaka, Y., M. Yamato, R. Imasu, and A. Ono, Transport of Asian dust (KOSA) particles; Importance of weak KOSA events on the geochemical cycle of soil particles, *Tellus, Ser. B*, *40*, 494–503, 1988.

Jaffe, D., T. Anderson, D. Covert, R. Kotchenruther, B. Trost, J. Danielson, W. Simpson, T. Berntsen, S. Karlsdottir, D. Blake, J. Harris, G. Carmichael, and I. Uno, Transport of Asian air pollution to North America, *Geophys. Res. Lett.*, *26*, 711–714, 1999.

Liu, Z., P. Voelger, and N. Sugimoto, Simulations of the observation of clouds and aerosols with the Experimental Lidar in Space Equipment (ELISE), *Appl. Opt.*, *39*(18), 3120–3137, 2000.

Liu, Z., N. Sugimoto, and T. Murayama, Extinction-to-backscatter ratio of Asian dust observed by high-spectral-resolution lidar and Raman lidar, *Appl. Opt.*, *41*(15), in press, 2002.

Murayama, T., N. Sugimoto, I. Uno, K. Kinoshita, K. Aoki, N. Hagiwara, Z. Liu, I. Matsui, T. Sakai, T. Shibata, K. Arao, B.-J. Shon, J.-G. Won, S.-C. Yoon, T. Li, J. Zhou, H. Hu, M. Abo, K. Iokibe, R. Koga, and Y. Iwasaka, Ground-based network observation of Asian dust events of April 1998 in east Asia, *J. Geophys. Res.*, *106*(D16), 18,345–18,359, 2001.

Sasano, Y., Tropospheric aerosol extinction coefficient profiles derived from scanning lidar measurements over Tsukuba, Japan from 1990 to 1993, *Appl. Opt.*, *35*(24), 4941–4952, 1996.

Sugimoto, N., I. Matsui, Z. Liu, A. Shimizu, I. Tamamushi, and K. Asai, Observation of aerosols and clouds using a two-wavelength polarization lidar during the Nauru99 experiment, *Sea and Sky*, *76*, 90–95, 2000.

Sugimoto, N., I. Matsui, Z. Liu, A. Shimizu, and K. Asai, Latitudinal distribution of aerosols and clouds in the western Pacific observed with a lidar on board the research vessel Mirai, *Geophys. Res. Lett.*, *28*, 4187–4190, 2001.

Uno, I., H. Amano, S. Emori, K. Kinoshita, I. Matsui, and N. Sugimoto, Trans-Pacific yellow sand transport observed in April 1998: A numerical simulation, *J. Geophys. Res.*, *106*(D16), 18,331–18,344, 2001a.

Uno, I., et al., Development and application of Chemical Weather Forecasting System over East Asia, 25th NATO/CCMS International Technical Meeting on Air Pollution Modeling and its Application, Oct. 2001b, (submitted).

N. Sugimoto, I. Matsui, and A. Shimizu, National Institute for Environmental Studies, 16-2 Onogawa, Tsukuba, Ibaraki 305-8506, Japan. (nsugimot@nies.go.jp; i-matsui@nies.go.jp; shimizua@nies.go.jp)

I. Uno, Research Institute for Applied Mechanics, Kyushu University, Kasuga Park 6-1, Kasuga, Fukuoka 816-8580, Japan.

K. Asai, Tohoku Institute of Technology, 35-1 Yagiyama-kasumicho, Taihaku-ku, Sendai, Miyagi 982-8577, Japan.

T. Endoh, Institute of Low Temperature Science, Hokkaido University, Kita-19, Nishi-8, Kisa-ku, Sapporo, Hokkaido 060-0819, Japan.

T. Nakajima, Center for Climate System Research, University of Tokyo, 4-6-1 Komaba, Meguro-ku, Tokyo 153-8904, Japan.